Alterations in chromatin at antigen receptor loci define lineage progression during B lymphopoiesis

Mattia Lion[a,b,1], Brejnev Muhire[a,b,1,2], Yuka Namiki[a,b], Michael Y. Tolstorukov[a,3,4], and Marjorie A. Oettinger[a,b,4]

[a]Department of Molecular Biology, Massachusetts General Hospital, Boston, MA 02114; and [b]Department of Genetics, Harvard Medical School, Boston, MA 02115

Edited by Gary Felsenfeld, National Institutes of Health, Bethesda, MD, and approved January 29, 2020 (received for review August 28, 2019)

Developing lymphocytes diversify their antigen receptor (AgR) loci by variable (diversity) joining (V[D]J) recombination. Here, using the micrococcal nuclease (MNase)-based chromatin accessibility (MACC) assay with low-cell count input, we profile both small-scale (kilobase) and large-scale (megabase) changes in chromatin accessibility and nucleosome occupancy in primary cells during lymphoid development, tracking the changes as different AgR loci become primed for recombination. The three distinct chromatin structures identified in this work define unique features of immunoglobulin H (IgH), Igκ, and T cell receptor-α (TCRα) loci during B lymphopoiesis. In particular, we find locus-specific temporal changes in accessibility both across megabase-long AgR loci and locally at the recombination signal sequences (RSSs). These changes seem to be regulated independently and can occur prior to lineage commitment. Large-scale changes in chromatin accessibility occur without significant change in nucleosome density and represent key features of AgR loci not previously described. We further identify local dynamic repositioning of individual RSS-associated nucleosomes at IgH and Igκ loci while they become primed for recombination during B cell commitment. These changes in chromatin at AgR loci are regulated in a locus-, lineage-, and stage-specific manner during B lymphopoiesis, serving either to facilitate or to impose a barrier to V(D)J recombination. We suggest that local and global changes in chromatin openness in concert with nucleosome occupancy and placement of histone modifications facilitate the temporal order of AgR recombination. Our data have implications for the organizing principles that govern assembly of these large loci as well as for mechanisms that might contribute to aberrant V(D)J recombination and the development of lymphoid tumors.

V(D)J recombination | chromatin accessibility | nucleosome positioning | B cell development | hematopoiesis

Antigen receptor (AgR) genes are assembled by a series of site-specific DNA rearrangement events. Variable (V), diversity (D), and joining (J) gene segments undergo recombination to form a functional gene encoding an AgR protein. These rearrangement events, collectively termed V(D)J recombination, are crucial for the formation of diverse immunoglobulin (Ig) and T cell receptor (TCR) repertoires (1).

AgR rearrangement is tissue specific (recombination occurs only in lymphocytes) as well as lineage specific such that rearrangement of TCR genes do not occur in B lymphocytes nor do complete rearrangements of Ig genes occur in T lymphocytes. Additionally, rearrangement is regulated with well-defined developmental-stage specificity such that, during B cell development, rearrangement of the IgH locus always precedes that of Ig light chains (2). Errors in the process can cause immunodeficiency syndromes and genome instability with the resulting potential for lymphoid malignancies (3–5).

Rearrangement at all seven AgR loci is mediated by the same recombination machinery (the RAG1/2 recombinase) in both B and T cells. The RAG recombinase initiates rearrangement by binding to conserved recombination signal sequences (RSSs) that flank each of the gene segments (1). Because the same recombination machinery is used for all recombination events, physical "accessibility" of RSSs to the RAG recombinase is a crucial level of regulation, and for over three decades, the accessibility hypothesis has been proposed to explain this type of regulation. The current model involves alterations in chromatin structure to explain the lineage specificity and temporal ordering of V(D)J recombination, but the nature of these changes remains poorly understood (1, 6).

The physical state of chromatin that determines accessibility of genomic DNA for integration with regulatory factors is defined by multiple components, including nucleosome positioning and occupancy, histone modifications, and DNA three-dimensional (3D) packaging as well as DNA methylation (7). Some of these features have been shown to correlate with V(D)J recombination, such as subnuclear repositioning, long-range AgR contraction, epigenetic marks, and cytosine–phosphate–guanine demethylation (8–11). In addition, our recent work (12) has shown that nucleosome positioning around the V RSSs is regulated in a cell-type and lineage-specific manner.

Chromatin accessibility and nucleosome occupancy are key and related (but distinct) features that orchestrate and regulate

Significance

Antigen receptor genes are assembled during lymphoid development from gene fragments by the process known as variable (diversity) joining (V[D]J) recombination. This process, which is initiated by the RAG1/RAG2 recombinase, is fundamental to the generation antigen receptor diversity required to respond to a virtually limitless array of pathogens. We show that chromatin at antigen receptor loci is subject to change during lymphoid development. We hypothesize that these developmentally regulated alterations of chromatin state may help to guide RAG1/RAG2 to the correct sites in recombinationally active cells. These changes represent key features of antigen receptor genes during lineage progression, serving either to facilitate or to impose a barrier to V(D)J recombination depending on cell lineage and developmental stage.

Author contributions: M.L., M.Y.T., and M.A.O. designed research; M.L., B.M., and Y.N. performed research; M.L. and B.M. analyzed data; and M.L., M.Y.T., and M.A.O. wrote the paper.

The authors declare no competing interest.

This article is a PNAS Direct Submission.

Data deposition: The raw and processed data reported in this paper have been deposited in the Gene Expression Omnibus (GEO) database, https://www.ncbi.nlm.nih.gov/geo (accession no. GSE132171).

[1]M.L. and B.M. contributed equally to this work.

[2]Present address: Center for Cancer and Cell Biology, Van Andel Research Institute, Grand Rapids, MI 49503.

[3]Present address: Department of Informatics and Analytics, Dana-Farber Cancer Institute, Boston, MA 02215.

[4]To whom correspondence may be addressed. Email: Michael_Tolstorukov@dfci.harvard.edu or oettinger@molbio.mgh.harvard.edu.

This article contains supporting information online at https://www.pnas.org/lookup/suppl/doi:10.1073/pnas.1914923117/-/DCSupplemental.

First published February 25, 2020.

gene expression (13). Here, we set out to identify changes in these properties at AgR loci during the development of B lymphocytes. We used a recently developed low-input version (14) of the MACC (micrococcal nuclease [MNase]-based chromatin accessibility) assay (15) that allowed for the simultaneous measurement of both chromatin opening and compaction as well as nucleosome occupancy. Measurement of all of these metrics in a single assay is a unique feature of MACC that fits the design of the current study. The MACC technique relies on a comparison of MNase sensitivity profiles (MNase-seq) obtained from a series of digestion depths, and it directly addresses the relationship between nucleosome occupancy and DNA accessibility. This approach provides a balanced metric of chromatin accessibility because the light digestion primarily profiles open genomic regions and the deep digestion primarily profiles closed regions. Moreover, previous methods could not profile chromatin accessibility both locally around the RSS and more globally across megabase-long AgR loci, limiting past analyses that used other techniques (16–18). Our assay has been successfully applied in both mammalian and *Drosophila* analyses (15, 19, 20). Our recent improved assay (14) was designed to profile low-abundance and rare cell populations, allowing for a profile of chromatin structure dynamics at AgR loci during B lymphopoiesis.

We find that chromatin openness is remodeled locally at RSSs and globally across AgR loci in a manner that correlates with the temporal order of V(D)J recombination. Moreover, distinct chromatin structures define important features of the IgH and Igκ loci during hematopoiesis and B cell development. In particular, a broadly high level of chromatin openness is observed globally across the entire IgH locus starting at the earliest stages of hematopoiesis prior to lineage commitment, while local opening at V_H RSSs occurs in a stepwise fashion that culminates at the B cell-biased lymphoid progenitor (BLP) stage where IgH recombination starts. For Igκ, both local opening around the Vκ RSS and global opening across the locus are restricted to the small pre–B cell stage when Igκ rearrangement is taking place. Nucleosome occupancy analysis similarly reveals dynamic changes during lymphoid development. In particular, a nucleosome spanning the RSSs for both IgH and Igκ is repositioned to a location in the coding region adjacent to the RSS during B cell commitment, consistent with the AgR recombination potential.

These results suggest that chromatin can be configured to be either permissive or repressive for V(D)J recombination during lymphoid development. We propose that both precise nucleosome positioning and local and global chromatin opening in concert with histone modifications and long-range contraction can facilitate RAG recombinase accessing the RSSs and can help regulate recombination order, fidelity, lineage restriction, and perhaps, allelic exclusion during V(D)J rearrangement. Our work provides an understanding of the changes in chromatin structure during B cell development in greater depth than has been available.

Results

Because of the low-abundance cell populations during B cell development, we recently developed a low-input version of the MACC assay (14) that allowed us to use ex vivo primary cells from wild-type C57BL/6 mice (*Materials and Methods*). The great advantage of this analysis is the possibility of interrogating chromatin accessibility changes in cell populations directly after sorting. Thus, results are not subject to potential sources of variation, such as those occurring when cells are cultured in the presence of feeder cells or cytokines. Information on both nucleosome positioning and chromatin accessibility is generated by the MACC assay. Additionally, the use of MACC has the great potential of profiling not only local and global regions of increased accessibility but also, regions that are repressed relative either to the surrounding chromatin or to the general level of accessibility genome wide.

The following populations were analyzed (Fig. 1*A* shows the developmental progression, and *SI Appendix*, Fig. S1*A* shows clustering of biological replicates): hematopoietic stem cells (HSCs); lymphoid-primed multipotent progenitors (LMPPs); common lymphoid "A"-type precursors (all-lymphoid progenitor, ALPs, or common lymphoid precursor, CLPs); BLPs [where D_H–J_H rearrangement occurs on both IgH alleles (21)]; B cell progenitors [pro-Bs; where V_H–DJ_H recombination occurs (22)]; large B cell precursors [large pre-Bs; that have undergone productive $V_HD_HJ_H$ rearrangement (22)]; and small B cell precursors [small pre-Bs; where Vκ–Jκ rearrangement happens (22)]. Lung epithelium cells were used as the control for nonlymphoid and recombinationally inactive cells. The recombination status of each cell population was confirmed by PCR and southern blotting (Fig. 1*B*).

Changes in Chromatin Accessibility at V_H RSSs Occur Stepwise during Early Stages of Hematopoiesis and B Cell Development. We first analyzed the chromatin status at V_H RSSs and found that these locations were marked by a progressive gain in openness (Fig. 1*C*). Surprisingly, a few V_H RSSs were already open at the pluripotent HSC stage prior to lineage commitment, while chromatin opening occurred at progressively more RSSs in multipotent LMPPs and lymphoid precursor ALPs. This progressive gain in chromatin accessibility around the RSSs culminates at the BLP stage where chromatin openness becomes a common feature at RSSs (Fig. 1*C* and *SI Appendix*, Fig. S1 *B–D*). The general background level of openness in the regions surrounding the RSSs was higher in BLPs than in the other cell types, reflecting the broadly higher level of openness across the entire locus (see below), but the spike in openness specifically around the RSSs is clearly evident (Fig. 1*C*). (We note that pro-B, large pre-B, and small pre-B stages are less informative because V_H segments have undergone recombination, deleting varying subsets of the segments. Thus, chromatin accessibility registered in these cell populations reflects openness from V_H segments that were retained after recombination or from unrearranged IgH loci.) We did not observe any peak of chromatin openness around V_H RSSs in lung epithelium cells, confirming the cell-type specificity of these changes. We instead observed a marked decrease of chromatin openness at the region adjacent to the RSS in the coding region of V_H segments in lung epithelium cells, which seemed to be a general phenomenon among V_H RSS (Fig. 1*C* and *SI Appendix*, Fig. S1 *B* and *C*), possibly reflecting a compacted structure.

Changes in Chromatin Accessibility at Vκ RSSs Occur at the Small Pre-B Stage. The pattern of chromatin opening around Vκ RSSs (Fig. 1*D*) was different from that observed at the IgH locus, confirming the developmental-stage specificity. Chromatin around Vκ RSSs is mainly silent in early progenitors and through the first stages of B cell commitment. However, at the small pre-B cell stage, where Vκ to Jκ rearrangement occurs, peaks of openness are found spanning the Vκ RSSs. Openness around Vκ RSSs appeared to be a common feature at RSSs, with opening occurring at all RSSs rather than in the more stepwise manner observed for IgH (*SI Appendix*, Figs. S1 *B–D* and S2 *A* and *B*). No change in openness was observed at Vκ RSSs in the control nonlymphoid lung epithelium.

At Vα, the average chromatin profiles (Fig. 1*E*) revealed that the RSSs were not open in any of the developmental stages investigated. However, a high level of openness was generally observed ∼1 kb upstream of the RSSs in LMPP, ALP, and BLP cells. This chromatin opening appears to be located around the promoter region of the Vα gene segments (see the average profile of chromatin openness around Vα TSSs) (*SI Appendix*, Fig. S2*C*). These changes precede TCRα germline transcription (23). We noted that this peak of chromatin openness disappeared

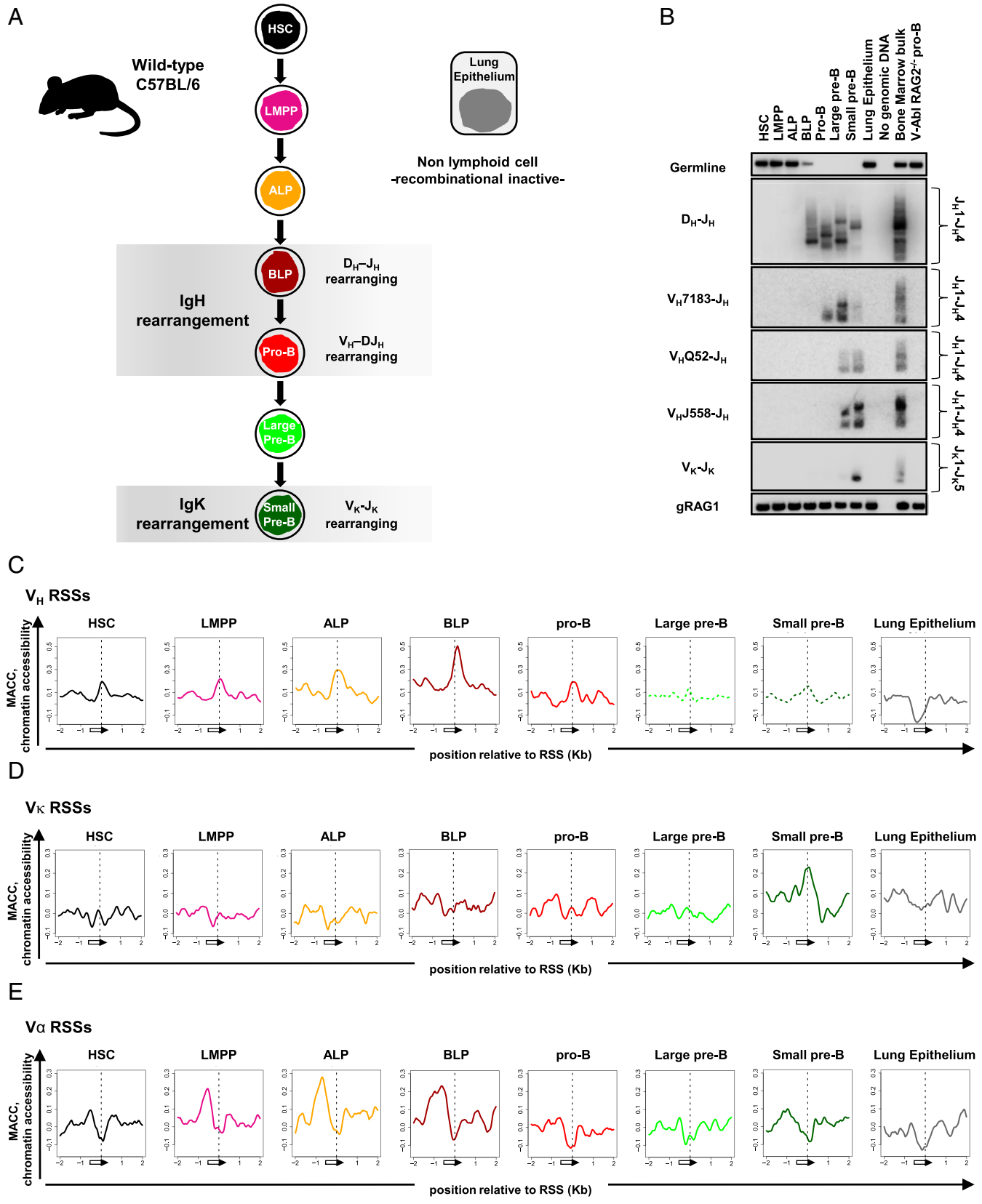

Fig. 1. B cell development is marked by stepwise changes of chromatin accessibility at V_H RSSs that precede the simultaneous opening of Vκ RSS at the small pre-B stage. (*A*) Schematic diagram of the hematopoietic differentiation stages included in this study (lung epithelium cells are also displayed). IgH and Igκ rearrangement steps are indicated. (*B*) Southern blot showing germline configuration and DJ_H, VDJ_H, and VJ_K joining (*Materials and Methods*). (*C–E*) Average profiles of chromatin accessibility around the 195 V_H RSSs (*C*), the 162 Vκ RSSs (*D*), and the 130 V_α RSSs (*E*; ±2 kb) of the cell populations depicted in *A*. Schematic representations of the RSS (black triangles) and its flanking V gene segment (white rectangles) are shown.

in committed B cell populations, suggesting stricter enforcement of developmental lineage specificity later on.

Analysis of chromatin opening at RSSs in cell lines confirmed that chromatin openness around V RSSs is subjected to cell-type regulation. We compared the chromatin from Abelson-transformed RAG2$^{-/-}$ pro-B cell lines where the Ig loci are in germline configuration but poised to undergo V(D)J recombination with that of nonlymphoid, recombinationally inactive RAG2$^{-/-}$ mouse embryonic fibroblasts (MEFs) (*Materials and Methods*). As shown in *SI Appendix*, Fig. S2*D*, chromatin around V_H and Vκ RSSs is highly accessible in pro-B cells, whereas MEFs show no gain in accessibility in their chromatin structure either around the RSSs or in the surrounding regions. In addition, in both cell types where the TCR genes are recombinationally inactive, the average profile of chromatin around Vα RSSs showed a background level of openness, with only a modest gain in accessibility at the Vα TSSs as noted above for primary cells (*SI Appendix*, Fig. S2 *C* and *D*).

As a validation of our approach, we confirmed that the average plots of chromatin accessibility at RSSs obtained using MACC were similar to the corresponding plots obtained using assay for transposase-accessible chromatin sequencing (ATAC-seq) data from the Immunological Genome (ImmGen) project (24) (*SI Appendix*, Fig. S2*E*). Of note, using MACC with primary small pre-B cells, we observed that the region upstream of Vκ RSSs (corresponding to the gene segment bodies and their promoter regions) showed high background levels of openness compared with the other cell types (Fig. 1*D*). The same region in the Rag2$^{-/-}$ pro-B cell line analysis and in the small pre-B cell ATAC-seq data presented a sharper and more defined peak of accessibility spanning the promoter region of the Vκ segments (*SI Appendix*, Fig. S2 *D* and *E*). Furthermore, our pro-B cell line MACC profiles (*SI Appendix*, Fig. S2*D*) were in agreement with previous DNase I hypersensitive sites sequencing analysis of RAG2$^{-/-}$ pro-B cells cultured in the presence of interleukin 7 (17, 18).

Together, these results support the accessibility hypothesis that puts forward changes in RSS openness as one of the mechanisms by which cell-, lineage-, and developmental-stage specificity is imposed on the recombination reaction.

Differential Regulation of Global Chromatin Openness across the IgH and Igκ Loci during Early Stages of Hematopoiesis and B-Lineage Commitment and Development. The MACC assay allows detection of both small-scale (hundreds of base pairs) and large-scale (megabase) changes in chromatin accessibility as the method permits profiling of continuous regions rather than being restricted only to sampling punctate peaks in accessibility (15). We, therefore, proceeded to the analysis of average chromatin openness (MACC value) at the entire AgR locus for IgH, Igκ, and TCRα. To evaluate the degree and significance of such openness, we compared the average MACC values of the AgR locus with the corresponding average MACC values estimated for 1,000 loci of the same size randomly selected across the rest of the chromosome where the AgR locus lies (*Materials and Methods* and *SI Appendix*, Fig. S3*A*). Our results proved consistent whether we used the median or mean MACC values within each compared genomic locus as highlighted in Fig. 2 *B* and *D* and *SI Appendix*, Fig. S3*B*.

While most of the V_H RSSs are not yet open in early HSCs, the overall chromatin structure of the entire IgH locus is significantly more open than expected by chance ($P = 0.001$) at this multipotent stage prior to lymphoid commitment (Fig. 2*A* shows genome browser profiles, and Fig. 2*B* shows permutation analysis). This open chromatin state is maintained throughout B cell development until the BLP stage, where it increases further. Hence, although chromatin across the entire IgH locus is already accessible in the early stages of hematopoiesis, we observed a locus-wide increase of its general level in BLPs ($P < 0.001$). No other regions of the same size as the IgH locus within chromosome 12 were comparably open. Thus, the chromatin structure at IgH locus seemed to be regulated such that it is maintained in a highly accessible state across the whole locus length. By contrast, the general level of IgH locus openness in lung epithelium cells was notably lower than that observed at B cell developmental stages (Fig. 2 *A* and *B*); however, the IgH locus was not closed significantly below the level of the average chromosomal state in these cells.

As we observed for the local openness around RSSs, the general level of chromatin openness across AgR loci during B cell development was regulated differently at the IgH and the Igκ loci. As shown in Fig. 2 *C* and *D*, chromatin at the Igκ locus was more closed than the chromosome-wide average in the first stages of hematopoiesis (HSC, LMPP, and ALP). During early stages of B cell commitment (BLP and following stages), there was a modest shift to a more open configuration at this locus followed by a dramatic increase at the small pre-B stage when Vκ to Jκ recombination occurs (Fig. 2*D*). Such an increase of chromatin openness across the whole Igκ locus in small pre-B cells is significant compared with other same-size regions within chromosome 6 ($P = 0.015$). While the level of accessibility of the Igκ locus in lung epithelium cells was somewhat higher than the chromosome-wide average, this effect was not statistically significant.

The level of chromatin opening estimated for the TCRα locus, a locus that is recombinationally silent in B cells, varied across interrogated cell types (*SI Appendix*, Fig. S3 *C* and *D*). The chromatin was significantly open in ALP and BLP cells, and its openness was reduced in lung epithelial cells. The levels of openness across the locus were not strongly correlated with local openness of chromatin around Vα RSSs (Fig. 1*E*), suggesting that local and global openings of the locus are regulated independently during development. As discussed above, this is also true for the IgH locus, where there is a discordance between local openness around the RSS and general openness across the locus.

Analysis of chromatin opening at AgR loci in RAG2$^{-/-}$ pro-B and MEF cell lines highlighted locus-wide, cell type-specific regulation. As shown in *SI Appendix*, Fig. S3*E*, we observed that chromatin openness at IgH, Igκ, and TCRα loci in MEFs was greatly reduced compared with regions outside AgR loci. Conversely, RAG2$^{-/-}$ pro-B cells showed high levels of openness across the whole IgH and Igκ loci. In particular, no other regions of the same size as the IgH locus within chromosome 12 were comparably open as similarly observed for BLPs (Fig. 2*B*). Analysis of the TCRα locus in the RAG2$^{-/-}$ pro-B cell line showed a higher than the chromosome-wide average openness, although not statistically significant (*SI Appendix*, Fig. S3*E*). Accessibility data at TCRα locus from both primary cells and cell lines would suggest that the global chromatin opening at AgR loci is not as strictly regulated in a lineage-specific manner as is the local openness around RSSs (Fig. 1*E* and *SI Appendix*, Figs. S2*D* and S3 *D* and *E*).

These large-scale changes in chromatin accessibility observed for IgH, Igκ, and TCRα loci occur without significant changes of nucleosome density (Fig. 2 *E* and *F* and *SI Appendix*, Fig. S3 *F* and *G*), with the exception of IgH locus in large and small pre-B cells (where recombination has deleted V_H segments in portions of the locus, which hinders reliable estimation of nucleosome density) (*SI Appendix*, Fig. S3 *F*, *Top*). Thus, as described previously in a different molecular system (20), we did not observe meaningful changes in averaged nucleosome density that could account for the changes in chromatin openness at AgR loci.

The observation that the chromatin structure of the entire IgH locus is already accessible at the HSC stage prior to lymphoid commitment is in direct contrast with 3D DNA fluorescence in situ hybridization data and subnuclear repositioning analysis of the IgH locus. Previous data have shown that the IgH locus relocates from the nuclear periphery to a more central location at the onset of B cell development, and this relocation is associated with chromatin opening and germline transcription of the V_H

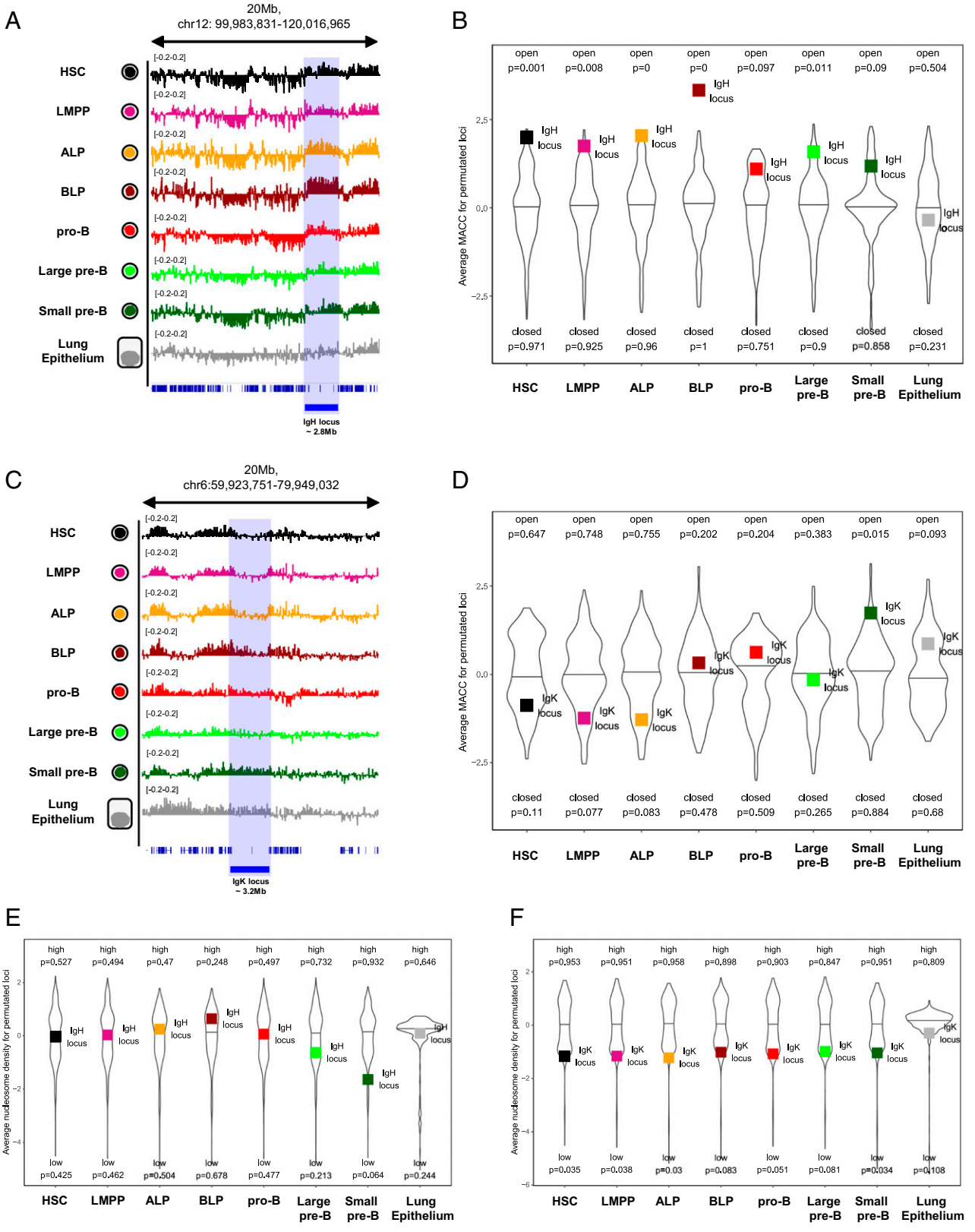

Fig. 2. Chromatin accessibility across the IgH and Igκ loci is regulated differently during hematopoiesis and B cell development. (*A* and *C*) Integrative Genomics Viewer (58) screenshots featuring accessibility across the entire IgH (~2.8 Mb) and Igκ (~3.2 Mb) locus of the cell populations depicted in Fig. 1*A*. Loci are shadowed in blue. AgR locus is depicted as a blue rectangle. (*B* and *D*) Assessment of the significance of chromatin accessibility at IgH (*B*) and Igκ (*D*) loci relative to accessibility across the chromosome (*Materials and Methods*). The violin plots represent the distribution of means of MACC values at simulated loci across the chromosome. The means of MACC values across IgH and Igκ loci are depicted as squares. *P* values of Wilcoxon test for median comparison of MACC distribution are indicated. (*E* and *F*) Assessment of the significance of nucleosome density at IgH (*E*) and Igκ (*F*) loci relative to the density across the chromosome was performed similarly to *B* and *D* (*Materials and Methods*).

genes in preparation for recombination (25–27). Although the nuclear periphery is believed to be a repressive compartment where chromatin is also in a repressive or inactive state (28), analysis of the publicly available ultralow-input RNA sequencing data from the ImmGen project (24) of a subset of cell types corresponding to the ones investigated in this manuscript revealed that some level of transcription across IgH locus precedes B cell commitment as early as HSC stage (genome browser profiles are shown in *SI Appendix*, Fig. S3 *H*, *Top*). Transcription across the IgH locus continued at the multipotent stage and the CLP stage and in all of the B cell types analyzed. Stromal medullary epithelial cells collected from the thymus were visualized as a nonlymphoid control and showed no detectable transcription across the locus (*SI Appendix*, Fig. S3 *H*, *Top*). Detection of transcription at the IgH locus at early stages of hematopoiesis is also in direct contrast with nuclear envelope association of the locus at these stages but supports our observation of chromatin openness at the IgH locus prior to B cell commitment and recombination. Visualization of transcription across the Igκ locus is also generally in agreement with our MACC data. No detectable levels of transcription in the more multipotent stages analyzed (HSC and multipotential progenitors) were observed, but modest levels of transcription were observed in CLP and prepro-B stages, and high levels were seen in pro-B and small pre-B cells (*SI Appendix*, Fig. S3 *H*, *Middle*). Again, the stromal epithelial cells showed no detectable transcription at IgK locus. The TCRα locus, by contrast, showed no variation in transcription across the cell types analyzed, with the exception of the control and small pre-B cells (*SI Appendix*, Fig. S3 *H*, *Bottom*). Overall, these observations would support that the chromatin structure at AgR loci is in a permissive state (*Discussion*).

The advantage of the MACC assay for detecting megabase-long domains of similar chromatin state has revealed information about these large AgR loci at distinct stages of lymphoid development. Taken together, these observations suggest that both global and local opening of chromatin are required for recombination to take place, underscoring the distinct layers of regulation of AgR accessibility.

RSS-Associated V_H and Vκ Nucleosomes Are Repositioned during B Cell Development. We used MNase-seq profiles from the MACC assay to compute nucleosome occupancy around the V RSSs of AgR loci. As a control, we computed nucleosome occupancy at CCCTC-binding factor sites, reproducing the expected profiles for all of the cell populations analyzed and confirming the robustness of our method (*Materials and Methods* and *SI Appendix*, Fig. S4*A*).

The average nucleosome occupancy plots show a well-positioned nucleosome spanning the V_H RSSs in both nonrecombining lymphoid cells and nonlymphoid cells (Fig. 3*A*). Strikingly, this stable nucleosome position was shifted during B cell development such that, at the BLP stage, it was adjacent to the V_H RSS in the coding region (the "−1 position"). In the ALP and pro-B stage, the location of the V_H nucleosome spanning the RSS appeared to shift toward the −1 position, suggesting that the nucleosome assumed an intermediate position at these developmental stages.

Nucleosomes appear to be positioned more loosely (or "fuzzy") around Vκ RSSs in nonlymphoid cells and cells prior to the large pre-B stage (in Fig. 3*B*, note the broad nucleosome occupancy region around the RSS). At the large pre-B stage, prior to Vκ to Jκ recombination, a more-defined nucleosome appears adjacent to the Vκ RSS in the −1 position followed by the appearance of a well-positioned −1 nucleosome in small pre-B cells when Vκ to Jκ recombination occurs.

Thus, in cells undergoing recombination (either the BLP or small pre-B stages for the IgH or Igκ loci, respectively), we observed a nucleosome positioned adjacent to the RSS in the coding region. In nonlymphoid and nonrecombining cell types, the RSS is occluded by nucleosomes in a similar manner either through the presence of a well-positioned nucleosome right at the RSS (IgH) or through the presence of loosely positioned nucleosomes around the RSS (Igκ).

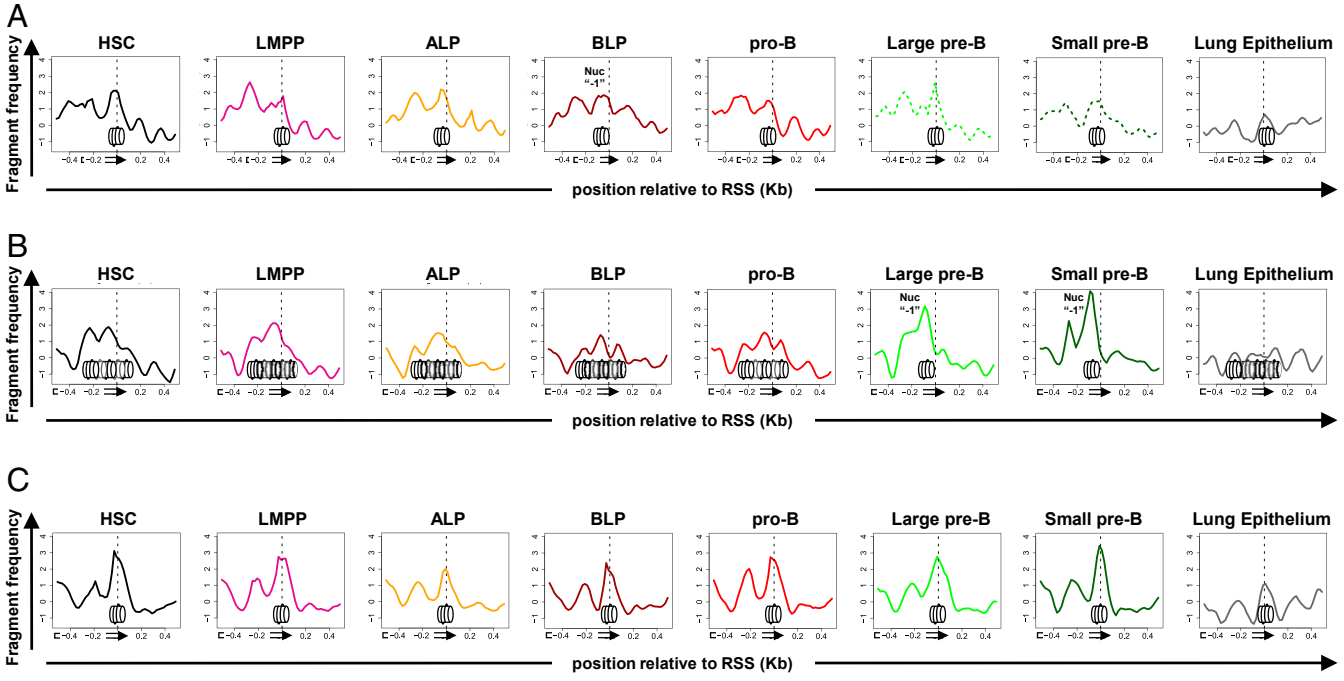

Fig. 3. Nucleosomes are repositioned around RSSs during B-lymphoid commitment. (*A*–*C*) Average profiles of nucleosome occupancy (*Materials and Methods*) around the 195 V_H RSSs (*A*), the 162 Vκ RSSs (*B*), and the 130 V_α RSSs (*C*; ±0.5 kb) of the cell populations depicted in Fig. 1*A*. Schematic representations of the RSS (black triangles), its flanking V gene segment (white rectangles), and the RSS-associated nucleosome are shown.

In keeping with the absence of recombination at Vα RSSs, analysis of nucleosome occupancy at these RSSs (Fig. 3*C*) showed that a well-positioned nucleosome was occluding the Vα RSSs, with the nucleosome centered around the RSS in all of the cell types analyzed.

Collectively, our results indicate that specific nucleosome placement around the V RSSs in developing B cells constitutes an additional regulatory layer for V(D)J rearrangement events. Together with other mechanisms of chromatin structure regulation described above, this layer enables stage- and lineage-specific control in line with our previous report (12).

Discussion

This study provides a profile of the serial changes in chromatin structure both across the Ig and TCR loci and at RSSs during early stages of hematopoiesis and B-lineage commitment and development. Such analysis was lacking in the V(D)J field, leaving open a series of questions about how and when alterations in chromatin structure would take place during lymphoid development at AgR loci. We showed that the lineage specificity and temporal ordering of gene rearrangements are correlated with the opening of chromatin broadly across the AgR loci and more locally around the RSSs. These changes in chromatin openness during B lymphopoiesis define unique features of IgH, Igκ, and TCRα loci. Furthermore, we observed that the RSS is occluded by a nucleosome in stages preceding recombination followed by the repositioning of the nucleosome to a site adjacent to the RSS in the coding region at the recombinationally active stage. These data suggest that chromatin structure modulates the accessibility of the RSS to the RAG proteins, serving either to facilitate or to impose a barrier to recombination depending on cell lineage and developmental stage.

Chromatin Accessibility Is Differentially Regulated across Different AgR Loci. We note that each locus presents a uniquely configured chromatin structure from restriction of openness to the small pre-B stage for the Igκ locus to maintenance of open chromatin structure throughout B cell commitment for the IgH locus (Fig. 2).

Furthermore, in the first stages of hematopoiesis prior to B cell commitment, reduced accessibility across the Igκ locus compared with surrounding regions outside the locus was observed (Fig. 2*C*). This reduction, although not accompanied by detectable transcription (*SI Appendix*, Fig. S3 *H*, *Middle*), does not result in the negative MACC scores of the magnitude detected at some other genomic regions (*SI Appendix*, Fig. S4*C*), suggesting only moderate levels of chromatin compaction. It is tempting to speculate that chromatin at the Igκ locus in HSCs, LMPPs, and ALPs may represent an intermediate "state" of "naïve" or "unprogrammed" chromatin, facilitating control and restriction of Igκ rearrangement while waiting for pioneer factors to initiate locus opening.

Global changes in chromatin opening at AgR loci were not perfectly synchronized with changes in chromatin that have been described during B cell development, such as changes in subnuclear positioning, locus contraction, and looping (11, 29). The presence of transcription across the IgH locus at early stages of hematopoiesis confirms that the chromatin at this locus must be in a permissive state. Whether transcription is a consequence of chromatin openness or chromatin opening is a consequence of transcription remains to be determined. It also remains to be determined whether changes in subnuclear positioning, locus contraction, and looping play a role in the dynamic changes in chromatin structure that we observe during lymphoid development or if they are separate events that act as distinct regulatory mechanisms.

Interestingly, nucleosome density across AgR loci does not vary during lymphoid development (Fig. 2 *E* and *F* and *SI Appendix*, Fig. S3 *F* and *G*), suggesting that molecular mechanisms other than "simple" nucleosome eviction are responsible for the increases in chromatin accessibility reported in this study. As an additional control, we confirmed that our approach can detect changes in nucleosome density in long genomic regions as shown in *SI Appendix*, Fig. S4 *D* and *E*, where nucleosome density of an ∼1-Mb region varies significantly across the cell types analyzed.

Chromatin Accessibility across AgR Loci and at RSS Is Temporally and Differentially Regulated. We observed that the timing of changes in chromatin accessibility at the RSS in relationship to opening of the entire AgR locus is not synchronized at the IgH and TCRα loci during B cell development (Figs. 1 *C* and *E* and 2*B* and *SI Appendix*, Fig. S3*D*). At these loci, chromatin becomes accessible on average locus wide while local chromatin at the RSSs is not yet open. This multistage opening could provide more regulatory control over the recombination process. Of note, in recombinationally inactive lung epithelium, global and local changes at the Igκ locus also seemed to be differentially regulated (Figs. 1*D* and 2*D*). Thus, the general level of chromatin accessibility at AgR loci may have a different function than local accessibility at RSS, but both seem to be required for a locus to be recombinationally competent (see the proposed model below).

Local Chromatin Openness Is Differentially Regulated at Different AgR V Segments. Analyses of a handful of chromatin properties at the Igκ locus including germline transcription and chromatin immunoprecipitation for several histone modifications and transcription factors using publicly available datasets obtained from pro-B cell lines have shown a bimodal distribution of these chromatin states at Vκ gene segments, corresponding to one peak at the promoter region and the other at the RSS of these segments (18). This difference in chromatin state distribution at Vκ gene segments may explain why, in the chromatin accessibility analysis presented here, we observed chromatin openness both around Vκ RSSs and Vκ promoter regions in small pre-B cells (Fig. 1*D*), Abelson-transformed RAG2$^{-/-}$ pro-B cells (*SI Appendix*, Fig. S2*D*), and with publicly available ATAC-seq data in small pre-B cells (*SI Appendix*, Fig. S2 *E*, *Middle*). Furthermore, this bimodal distribution in chromatin states is in contrast to the absence of such a distribution at the IgH locus where active chromatin states are only present in the V_H RSS region (17, 18), again confirming our observations of the chromatin openness distribution at V_H RSSs (Fig. 1*C* and *SI Appendix*, Fig. S2 *D* and *E*, *Top*).

Dynamic Nucleosomes Participate in Temporal- and Lineage-Specific Control of V(D)J Recombination. The use of MNase digestion of chromatin followed by high-throughput sequencing (MNase-seq) is the most widely used nucleosome mapping method. To further confirm that we were primarily measuring nucleosomes, we plotted the distribution of digestion fragment lengths (*SI Appendix*, Fig. S4*B*). As expected (30, 31), these plots showed that overdigestion at high MNase concentration (both genome wide and at regions surrounding the RSSs) occurs in ∼10-bp steps, which are specific to nucleosomes (and not to other complexes with similar DNA protection size). Moreover, unlike the situations where site-specific binding proteins might mimic the observed nucleosomal protection, the nucleosome density profiles that we mapped reveal nucleosome repositioning in a characteristic developmental pattern. Such specific repositioning would be far more consistent with the known ability of nucleosomes to be specifically moved rather than other nucleosome-sized complexes assembling at different sites.

The nucleosome occupancy data presented here expand our understanding of the multiple roles that the nucleosome seems to play in the regulation of V(D)J recombination. In vitro studies have showed that assembly of RSSs into nucleosomes inhibits V(D)J recombination (32–35), supporting the idea that nucleosomes are intrinsically inhibitory to DNA cleavage by RAG recombinase.

At the same time, binding of RAG2 to H3 trimethylation at lysine 4 (H3K4me3) is required for V(D)J recombination in vivo

and is thought to enhance the catalytic activity of the RAG complex (8, 36–39). Our recent work with RAG-deficient pro-T, pro-B, and fibroblastoid cell lines (12) has suggested a dual role for nucleosomes: 1) regulating access to the RSS and 2) activating RAG function through the interaction of RAG2 with H3K4me3. Here, using purified ex vivo cells during B-lymphocyte development, we probe in detail the nucleosomal landscape around RSSs, showing that nucleosome placement occludes the RSS in cells where recombination does not occur, while a nucleosome occupies the RSS-adjacent −1 position as cells prepare for recombination during lymphoid development (Fig. 3). These observations fit with our previous work and suggest that nucleosome positioning can play a crucial role in governing V(D)J recombination through the developmental stage- and lineage-specific positioning around the RSS of the V segments.

We also note that nucleosome repositioning and the change in local openness are not simultaneous, suggesting that they represent two distinct levels of regulation. For example, nucleosome repositioning around Vκ RSSs in large pre-B cells is not accompanied by changes in chromatin accessibility in these cells (Figs. 1*D* and 3*B*). Rather, openness of the chromatin at the RSS follows nucleosome repositioning.

Chromatin Structure Analysis Provides Implications for RAG Scanning Mechanism. Recent studies (3, 40, 41) have proposed a linear chromatin scanning activity for RAG proteins that could work in place of or in combination with diffusion-related mechanisms (42). RAG linear scanning from the recombinational center is thought to occur over chromatin in order to capture a V RSS, a process that could be mediated by chromatin loop extrusion (43). The current measures of chromatin accessibility do not adequately capture enough features to speculate about epigenetic mechanisms underlying lineage- and stage-specific regulation of AgR rearrangement. Based on our MACC analysis that profiles local and global regions of increased and repressed accessibility as well as nucleosome occupancy, we provide additional insights into this proposed RAG scanning mechanism. In particular, we propose a working model (Fig. 4) where the RAG complex would initially scan open chromatin locus wide to locate its target through the use of local peaks of chromatin accessibility at V RSSs. This in concert with the specific nucleosome positioning pattern at the V RSS and placement of the epigenetic modification H3K4me3 would favor rearrangement with the recombination center. Our results suggest that the general level of accessibility across the AgR locus is among the first features required for "priming" the locus for recombination, playing a "pioneer" role. These changes in chromatin openness across megabase-long domains represent key features of AgR loci not previously described and difficult to profile with the use of other techniques. We suggest that locus-wide openness is a required step that is necessary along with local opening around RSSs in order for the RAG recombinase to properly access the RSS. The presence of a nucleosome (that may display H3K4me3) adjacent to the RSS in the coding region of the V segment would ensure that RSS is unprotected for cleavage; this helps to direct the recombinase

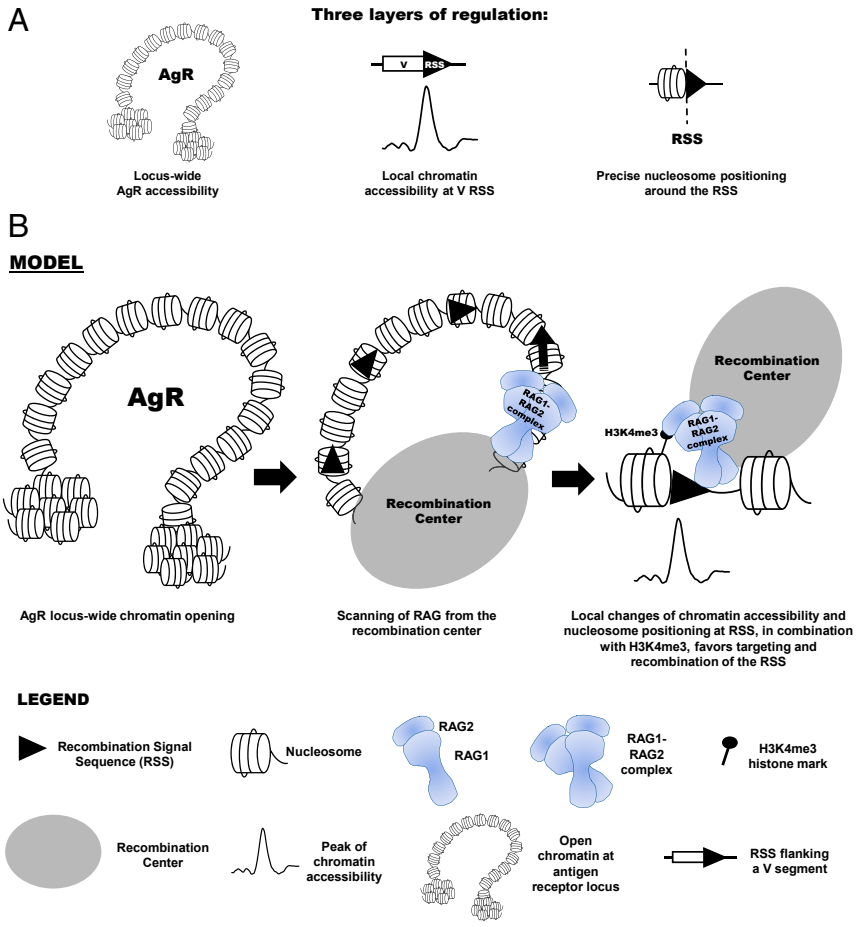

Fig. 4. Combination of three layers of chromatin regulation facilitates accessibility of AgR loci to the recombinase machinery. (*A*) Schematic representation of the three layers of chromatin regulation discussed in this paper: global changes in chromatin openness, local changes in openness, and regulation of precise nucleosome positioning. (*B*) Working model for potential roles of chromatin accessibility and nucleosome positioning during V(D)J recombination (*Discussion*).

specifically to RSS, facilitating faithful regulation of the rearrangement events. Presence of these multiple layers of regulation could also help to reconcile why RAG activity is restricted specifically to AgR loci at the right developmental stages, despite binding to thousands of sites in the genome (5).

Together, our data provide insights into how the RAG proteins are recruited at AgR loci to ensure lineage- and developmental-stage specificity and have implications for the organizing principles that govern assembly of these large loci and for mechanisms that might contribute to aberrant recombination events and the development of lymphoid tumors. The combination of the three layers of chromatin regulation discussed in this paper—global changes in chromatin openness, local changes in openness, and regulation of precise nucleosome positioning (Fig. 4*A*)—may be a more general mechanism by which cells can modulate accessibility of their genomic DNA for interaction with protein factors during development.

Materials and Methods

Cell Culture. $Rag2^{-/-}$ pro-B Abelson-transformed cell lines and $Rag2^{-/-}$ MEFs were generated from Rag2-deficient C57BL/6N mice obtained from Taconic Biosciences as previously described (12). The pro-B cell line was maintained in RPMI-1640 medium (Sigma-Aldrich) supplemented with 10% HyClone bovine calf serum (Fisher Scientific), 1% penicillin/streptomycin/L-glutamine (Fisher Scientific), and 0.05 mM 2-mercaptoethanol (Gibco). MEFs were maintained in DMEM-11995 medium (Gibco) supplemented with 10% HyClone bovine calf serum and 1% penicillin/streptomycin/L-glutamine.

Mice. Wild-type C57BL/6N mice (4 to 6 wk old) were purchased from Taconic Biosciences. All animal procedures were performed according to NIH guidelines and approved by the Committee on Animal Care at Massachusetts General Hospital and Harvard University.

Primary Cell Isolation and Sorting. Bone marrow cells were isolated and immunolabeled as previously described (44). Briefly, bone marrow cell suspensions from tibias, femurs, hips, and spines of 4- to 6-wk-old wild-type C57BL/6N mice were collected, and red blood cells were lysed with ammonium–chloride–potassium lysing buffer (150 mM NH_4Cl, 10 mM $KHCO_3$, 0.1 mM ethylenediaminetetraacetic acid [EDTA]). Lineage-positive cells were subsequently resuspended in staining medium (1% bovine serum albumin/1 mM EDTA/phosphate-buffered saline [PBS]), labeled, and removed with magnetic beads (*Gating Strategy for Cell Populations*). Lineage-negative cells were labeled according to our gating strategy and resuspended in staining medium without EDTA for sorting analysis.

Lungs were collected and processed as previously described (45). Briefly, lungs were chopped into small pieces in 2% fetal calf serum (FCS)/PBS media and washed several times. Lung pieces were incubated in PBS with Ca^{2+} and Mg^{2+} for 30 min at 37 °C in collagenase type IV (200 U/mL). Supernatant was collected and washed in 2% FCS/PBS media. Pellet was resuspended in Gibco Trypsin-EDTA (Thermo Fisher Scientific) and digested for 10 min at 37 °C. Supernatant was collected and washed in 2% FCS/PBS media. Undigested lung was smashed on the strainer in 2% FCS/PBS media. Cells were labeled according to our gating strategy and resuspended in staining medium without EDTA for sorting analysis

A five-laser cell sorter FACSAria-III (BD) was used for cell sorting, and cells were collected in 10% fetal bovine serum/PBS. Subsequent analysis was performed using FlowJo software.

Gating Strategy for Cell Populations. HSCs and LMPPs were isolated as previously described (44). Briefly, lineage depletion was carried out by removal with magnetic beads conjugated to BioMag goat anti-rat IgG (Qiagen 310107) of the following marker antibodies: Ter119, B220, CD19, Mac-1, Gr-1, IgM, CD3, CD8a, and DX5. Lineage-negative cells were stained with the following antibodies: HSC (Lin^-, $cKit^+$, $Sca\text{-}1^{int/+}$, $CD34^+$, $FLT3^-$) and LMPP (Lin^-, $cKit^+$, $Sca\text{-}1^{int/+}$, $CD34^+$, $FLT3^+$).

ALPs (or CLPs) and BLPs were isolated as previously described (46–48). Briefly, after lineage depletion (Ter119, Mac-1, B220, Gr-1, CD3e; biotin anti-mouse lineage panel Biolegend 133307), bone marrow cells were stained as followed: ALP (Lin^-, $cKit^{mid/lo}$, $IL7Ra^+$, $Sca\text{-}1^{lo}$, $FLT3^+$, $Ly6D^-$) and BLP (Lin^-, $cKit^{mid/lo}$, $IL7Ra^+$, $Sca\text{-}1^{lo}$, $FLT3^{+/int}$, $Ly6D^+$).

Pro-B, large pre-B, and small pre-B cells were isolated as previously described (49, 50). Bone marrow cells were stained as followed: pro-B ($CD19^+$, IgM^-, $cKit^{lo}$, $CD43^+$), large pre-B ($CD19^+$, IgM^-, $cKit^-$, $CD43^{+/-}$, $CD2^-$), and small pre-B ($CD19^+$, IgM^-, $cKit^-$, $CD43^-$, $CD2^+$).

Lung epithelium cells were stained as followed: $CD326\ (EpCam)^+$, $CD19^-$, $CD3^-$, and $CD45^-$.

Postsort analysis confirmed purity of cell fractions.

V(D)J Assay and Southern Blot. Genomic DNA was purified from sorted cell populations. PCR assays for D_H to J_H, V_H to DJ_H, or Vκ to Jκ rearrangements were adapted from ref. 51 to work with 1 ng of total material. Briefly, PCR was set according to the NEBNext Q5 Hot Start HiFi PCR Master Mix (New England Biolabs) manufacturing protocol. PCR products were analyzed on an agarose gel, blotted to Amersham Hybond-N+ membrane (GE Healthcare), and followed by southern blotting.

Southern blot was carried out as previously described (52). Briefly, blots were prehybridized at 42 °C for 1 h and then, hybridized overnight using a P^{32} end-labeled oligonucleotide probe. Blots were washed with 2× saline-sodium citrate + 0.05% sodium dodecyl sulfate (SDS) for 20 min four times, and radioactive signals were detected by a GE Healthcare Amersham Typhoon imager. The nonrearranging RAG1 locus served as a loading control. Lane 9 is an amplification reaction with no genomic DNA. Samples in lanes 10 and 11 were used as controls: whole wild-type C57BL/6N bone marrow extract and Abelson-transformed $RAG2^{-/-}$ pro-B lymphocytes.

Low-Input MACC Assay and Library Preparation. Low-input MACC assay was performed as previously described (14). Briefly, cells were collected after cell sorting, and nuclei were extracted using 1 vol of 2× nuclei extraction buffer (0.6 M sucrose, 4 mM $MgOAc_2$, 2% Triton X-100, 20 mM Hepes [4-(2-hydroxyethyl)-1-piperazineethanesulfonic acid], pH 7.8, 2 mM $CaCl_2$, 8 mM $MgCl_2$). Nuclei were counted and subjected to digestion with titrated amounts of MNase (Worthington) for 5 min at 37 °C. The following numbers of nuclei were used for each titration point: 2,500 (HSC), 5,000 (LMPP), 2,500 (CLP), 1,250 (BLP), 2,500 (pro-B), 5,000 (large pre-B), 5,000 (small pre-B), and 2,000 (lung epithelium). Reactions were terminated with 50 mM EDTA/ethylene glycol-bis(β-aminoethyl ether)-*N*,*N*,*N*′,*N*′-tetraacetic acid. MNase-digested samples were treated with 500 μg/mL RNase A (Thermo Fisher Scientific) for 1 h at 37 °C and incubated with 1 mg/mL proteinase K (Ambion) and 1% SDS overnight at 60 °C. Digested DNA was cleaned up using Agencourt AMPure XP beads (Beckman Coulter) and visualized on either Agilent Bioanalyzer or Agilent TapeStation.

Libraries were prepared for each individual titration point using the NEBNext Ultra II DNA Library Prep Kit for Illumina (New England Biolabs) and barcoded using NEBNext Multiplex Oligos for Illumina (Index Primers Set 1&2; New England Biolabs). Number of PCR cycles was calculated using a real-time qPCR-based approach (53). Four barcoded titration libraries were pooled in one sample, and paired-end 50-cycle sequencing in an Illumina HiSeq 2500 instrument was performed.

Data Preprocessing and Computation of MACC Profiles. Sequenced paired-end reads were mapped to mouse genome (mm10) using Bowtie aligner v. 0.12.9 (54), with insert size between 50 and 500 bp. Reads with both pair mates aligned to the same genomic positions at high frequency (above z score = 7) were considered anomalous and were filtered out (55). The centers of the sequenced fragments were counted in 300-bp bins genome wide for each of the two MNase titration points and each of the two independent biological replicates. Fragment counts for each sample were normalized for library size and multiplied by 10^6 to obtain "fragments per million mapped" frequencies. Obtained fragment frequencies were averaged between replicates, and MACC scores were computed as described before (15, 56). Specifically, at every 300-bp bin, we fitted a straight line between fragment frequencies corresponding to the lowest and highest titrations. Then, the slope of the line at every bin was corrected using a method based on locally weighted scatterplot smoothing to address the potential bias due to the variability of the guanine–cytosine content of the underlying sequence, and the obtained values were used as MACC scores.

Estimation of Significance of Chromatin Accessibility and Nucleosome Density at AgR Loci. To assess the significance of chromatin accessibility at a particular AgR locus, we applied a permutation-based test that evaluates accessibility of the locus relative to the rest of the chromosome. Specifically, we randomly sampled 1,000 regions (of the same size as the AgR locus analyzed) on the same chromosome, excluding the AgR locus itself. MACC values within the bins across the AgR locus were compared with those computed for the bins in each sampled region using Wilcoxon test (significance threshold $P < 0.05$). Values were transformed into z scores, and the resulted profiles were plotted. Empirical permutation P values for "openness" (or "closeness") of AgR locus were calculated as the fractions of occurrences when the sampled regions were significantly more (or less) accessible than the AgR locus (*SI Appendix*, Fig. S3*A*).

A similar permutation-based test was used to assess the changes in nucleosome density. Fragments were counted in 300-bp bins, and the obtained

values were normalized for library size and aggregated over the lowest and highest titration points. Each locus was compared with 1,000 randomly regions (of the same size as the AgR locus analyzed) on the same chromosome, excluding the AgR locus itself. Values were transformed into *z* scores, and the resulted profiles were plotted. For each cell type, the two *P* values computed (Wilcoxon test) indicate significance of high and low nucleosome density.

Nucleosome Positioning. Nucleosome occupancy analysis was carried out as previously described (57). Briefly, for every cell type, normalized fragment frequencies in the 300-bp bins were aggregated over the lowest and highest titration points. Average nucleosome occupancy profiles were computed by averaging the scores over all of the V RSSs of an AgR locus. The average occupancy values were transformed into *z* scores, and the resulted profiles were plotted ±0.5 kb around the V RSSs.

Data Availability. Raw and processed data have been deposited in the Gene Expression Omnibus (GEO) database, https://www.ncbi.nlm.nih.gov/geo, under accession number GSE132171.

ACKNOWLEDGMENTS. We thank Dr. Katia Georgopoulos and Dr. Toshimi Yoshida (Harvard Medical School) for comments and help with the cell-sorting strategy. We thank Dr. Robert E. Kingston (Harvard Medical School) for insightful discussions and comments on the manuscript. This work was in part supported by the Harvard Medical School Epigenetics Seed Grant.

1. A. J. Little, A. Matthews, M. Oettinger, D. B. Roth, D. G. Schatz, "The mechanism of V(D)J recombination" in *Molecular Biology of B Cells*, F. W. Alt, T. Honjo, A. Radbruch, M. Reth, Eds. (Elsevier Ltd, Amsterdam, Netherlands, ed. 2, 2015), pp. 13–34.
2. A. G. W. Matthews, M. A. Oettinger, RAG: A recombinase diversified. *Nat. Immunol.* **10**, 817–821 (2009).
3. J. Hu *et al*., Chromosomal loop domains direct the recombination of antigen receptor genes. *Cell* **163**, 947–959 (2015).
4. M. Mijušković *et al*., Off-target V(D)J recombination drives lymphomagenesis and is escalated by loss of the Rag2 C terminus. *Cell Rep.* **12**, 1842–1852 (2015).
5. G. Teng *et al*., RAG represents a widespread threat to the lymphocyte genome. *Cell* **162**, 751–765 (2015).
6. D. Jung, C. Giallourakis, R. Mostoslavsky, F. W. Alt, Mechanism and control of V(D)J recombination at the immunoglobulin heavy chain locus. *Annu. Rev. Immunol.* **24**, 541–570 (2006).
7. L. Holtzman, C. A. Gersbach, Editing the epigenome: Reshaping the genomic landscape. *Annu. Rev. Genomics Hum. Genet.* **19**, 43–71 (2018).
8. A. G. W. Matthews *et al*., RAG2 PHD finger couples histone H3 lysine 4 trimethylation with V(D)J recombination. *Nature* **450**, 1106–1110 (2007).
9. R. Selimyan *et al*., Localized DNA demethylation at recombination intermediates during immunoglobulin heavy chain gene assembly. *PLoS Biol.* **11**, e1001475 (2013).
10. M. Busslinger, A. Tarakhovsky, Epigenetic control of immunity. *Cold Spring Harb. Perspect. Biol.* **6**, 1–28 (2014).
11. C. Proudhon, B. Hao, R. Raviram, J. Chaumeil, J. A. Skok, Long-range regulation of V(D)J recombination. *Adv. Immunol.* **128**, 123–182 (2015).
12. S. R. Pulivarthy *et al*., Regulated large-scale nucleosome density patterns and precise nucleosome positioning correlate with V(D)J recombination. *Proc. Natl. Acad. Sci. U.S.A.* **113**, E6427–E6436 (2016).
13. W. K. M. Lai, B. F. Pugh, Understanding nucleosome dynamics and their links to gene expression and DNA replication. *Nat. Rev. Mol. Cell Biol.* **18**, 548–562 (2017).
14. M. Lion, M. Y. Tolstorukov, M. A. Oettinger, Low-input MNase accessibility of chromatin (Low-Input MACC). *Curr. Protoc. Mol. Biol.* **127**, e91 (2019).
15. J. Mieczkowski *et al*., MNase titration reveals differences between nucleosome occupancy and chromatin accessibility. *Nat. Commun.* **7**, 11485 (2016).
16. M. Mandal *et al*., Histone reader BRWD1 targets and restricts recombination to the Igk locus. *Nat. Immunol.* **16**, 1094–1103 (2015).
17. D. J. Bolland *et al*., Two mutually exclusive local chromatin states drive efficient V(D)J recombination. *Cell Rep.* **15**, 2475–2487 (2016).
18. L. S. Matheson *et al*., Local chromatin features including PU.1 and IKAROS binding and H3K4 methylation shape the repertoire of immunoglobulin kappa genes chosen for V(D)J recombination. *Front. Immunol.* **8**, 1550 (2017).
19. A. M. Deaton *et al*., Enhancer regions show high histone H3.3 turnover that changes during differentiation. *eLife* **5**, e15316 (2016).
20. B. Mueller *et al*., Widespread changes in nucleosome accessibility without changes in nucleosome occupancy during a rapid transcriptional induction. *Genes Dev.* **31**, 451–462 (2017).
21. C. Bossen *et al*., The chromatin remodeler Brg1 activates enhancer repertoires to establish B cell identity and modulate cell growth. *Nat. Immunol.* **16**, 775–784 (2015).
22. K. Georgopoulos, The making of a lymphocyte: The choice among disparate cell fates and the IKAROS enigma. *Genes Dev.* **31**, 439–450 (2017).
23. B. del Blanco, Ú. Angulo, M. S. Krangel, C. Hernández-Munain, T-cell receptor α enhancer is inactivated in αβ T lymphocytes. *Proc. Natl. Acad. Sci. U.S.A.* **112**, E1744–E1753 (2015).
24. H. Yoshida *et al*.; Immunological Genome Project, The cis-regulatory atlas of the mouse immune system. *Cell* **176**, 897–912.e20 (2019).
25. S. T. Kosak *et al*., Subnuclear compartmentalization of immunoglobulin loci during lymphocyte development. *Science* **296**, 158–162 (2002).
26. M. Fuxa *et al*., Pax5 induces V-to-DJ rearrangements and locus contraction of the immunoglobulin heavy-chain gene. *Genes Dev.* **18**, 411–422 (2004).
27. E. Roldán *et al*., Locus 'decontraction' and centromeric recruitment contribute to allelic exclusion of the immunoglobulin heavy-chain gene. *Nat. Immunol.* **6**, 31–41 (2005).
28. E. Deniaud, W. A. Bickmore, Transcription and the nuclear periphery: Edge of darkness? *Curr. Opin. Genet. Dev.* **19**, 187–191 (2009).
29. A. L. Kenter, A. J. Feeney, New insights emerge as antibody repertoire diversification meets chromosome conformation. *F1000 Res.* **8**, 347 (2019).
30. D. Riley, H. Weintraub, Nucleosomal DNA is digested to repeats of 10 bases by exonuclease III. *Cell* **13**, 281–293 (1978).
31. R. V. Chereji, T. D. Bryson, S. Henikoff, Quantitative MNase-seq accurately maps nucleosome occupancy levels. *Genome Biol.* **20**, 198 (2019).
32. J. Kwon, A. N. Imbalzano, A. Matthews, M. A. Oettinger, Accessibility of nucleosomal DNA to V(D)J cleavage is modulated by RSS positioning and HMG1. *Mol. Cell* **2**, 829–839 (1998).
33. J. Kwon, K. B. Morshead, J. R. Guyon, R. E. Kingston, M. A. Oettinger, Histone acetylation and hSWI/SNF remodeling act in concert to stimulate V(D)J cleavage of nucleosomal DNA. *Mol. Cell* **6**, 1037–1048 (2000).
34. A. Golding, S. Chandler, E. Ballestar, A. P. Wolffe, M. S. Schlissel, Nucleosome structure completely inhibits in vitro cleavage by the V(D)J recombinase. *EMBO J.* **18**, 3712–3723 (1999).
35. F. McBlane, J. Boyes, Stimulation of V(D)J recombination by histone acetylation. *Curr. Biol.* **10**, 483–486 (2000).
36. Y. Liu, R. Subrahmanyam, T. Chakraborty, R. Sen, S. Desiderio, A plant homeodomain in RAG-2 that binds Hypermethylated lysine 4 of histone H3 is necessary for efficient antigen-receptor-gene rearrangement. *Immunity* **27**, 561–571 (2007).
37. N. Shimazaki, A. G. Tsai, M. R. Lieber, H3K4me3 stimulates the V(D)J RAG complex for both nicking and hairpinning in trans in addition to tethering in cis: Implications for translocations. *Mol. Cell* **34**, 535–544 (2009).
38. J. Bettridge, C. H. Na, A. Pandey, S. Desiderio, H3K4me3 induces allosteric conformational changes in the DNA-binding and catalytic regions of the V(D)J recombinase. *Proc. Natl. Acad. Sci. U.S.A.* **114**, 1904–1909 (2017).
39. G. J. Grundy, W. Yang, M. Gellert, Autoinhibition of DNA cleavage mediated by RAG1 and RAG2 is overcome by an epigenetic signal in V(D)J recombination. *Proc. Natl. Acad. Sci. U.S.A.* **107**, 22487–22492 (2010).
40. S. Jain, Z. Ba, Y. Zhang, H. Q. Dai, F. W. Alt, CTCF-binding elements mediate accessibility of RAG substrates during chromatin scanning. *Cell* **174**, 102–116.e14 (2018).
41. Y. Zhang *et al*., The fundamental role of chromatin loop extrusion in physiological V(D)J recombination. *Nature* **573**, 600–604 (2019).
42. J. S. Lucas, Y. Zhang, O. K. Dudko, C. Murre, 3D trajectories adopted by coding and regulatory DNA elements: First-passage times for genomic interactions. *Cell* **158**, 339–352 (2014).
43. S. G. Lin, Z. Ba, F. W. Alt, Y. Zhang, RAG chromatin scanning during V(D)J recombination and chromatin loop extrusion are related processes. *Adv. Immunol.* **139**, 93–135 (2018).
44. T. Yoshida, S. Y. Ng, J. C. Zuniga-Pflucker, K. Georgopoulos, Early hematopoietic lineage restrictions directed by Ikaros. *Nat. Immunol.* **7**, 382–391 (2006).
45. M. Vanlandewijck, J. Andrae, L. Gouveia, C. Betsholtz, Preparation of single cell suspensions from the adult mouse lung. *Protoc. Exch.*, 10.1038/protex.2018.006 (2018).
46. R. Revilla-I-Domingo *et al*., The B-cell identity factor Pax5 regulates distinct transcriptional programmes in early and late B lymphopoiesis. *EMBO J.* **31**, 3130–3146 (2012).
47. E. V. Rothenberg, Transcriptional control of early T and B cell developmental choices. *Annu. Rev. Immunol.* **32**, 283–321 (2014).
48. M. Miyazaki *et al*., The E-Id protein axis specifies adaptive lymphoid cell identity and suppresses thymic innate lymphoid cell development. *Immunity* **46**, 818–834.e4 (2017).
49. I. Joshi *et al*., Loss of Ikaros DNA-binding function confers integrin-dependent survival on pre-B cells and progression to acute lymphoblastic leukemia. *Nat. Immunol.* **15**, 294–304 (2014).
50. Y. Hu *et al*., Superenhancer reprogramming drives a B-cell-epithelial transition and high-risk leukemia. *Genes Dev.* **30**, 1971–1990 (2016).
51. M. S. Schlissel, L. M. Corcoran, D. Baltimore, Virus-transformed pre-B cells show ordered activation but not inactivation of immunoglobulin gene rearrangement and transcription. *J. Exp. Med.* **173**, 711–720 (1991).
52. C. C. Giallourakis *et al*., Elements between the IgH variable (V) and diversity (D) clusters influence antisense transcription and lineage-specific V(D)J recombination. *Proc. Natl. Acad. Sci. U.S.A.* **107**, 22207–22212 (2010).
53. S. K. Bowman *et al*., Multiplexed Illumina sequencing libraries from picogram quantities of DNA. *BMC Genomics* **14**, 466 (2013).
54. B. Langmead, C. Trapnell, M. Pop, S. L. Salzberg, Ultrafast and memory-efficient alignment of short DNA sequences to the human genome. *Genome Biol.* **10**, R25 (2009).
55. P. V. Kharchenko, M. Y. Tolstorukov, P. J. Park, Design and analysis of ChIP-seq experiments for DNA-binding proteins. *Nat. Biotechnol.* **26**, 1351–1359 (2008).
56. A. Cook, J. Mieczkowski, M. Y. Tolstorukov, Single-assay profiling of nucleosome occupancy and chromatin accessibility. *Curr. Protoc. Mol. Biol.* **120**, 21.34.1–21.34.18 (2017).
57. J. Mieczkowski, M. Y. Tolstorukov, "Bioinformatic analysis of nucleosome and histone variant positioning" in *Histone Variants: Methods and Protocols*, G. A. Orsi, G. Almouzni, Eds. (Springer, New York, 2018), pp. 185–203.
58. J. T. Robinson *et al*., Integrative genomics viewer. *Nat. Biotechnol.* **29**, 24–26 (2011).